ChemSusChem

Energy storage in strained organic molecules: Electrochemical and spectroelectrochemical characterization of norbornadiene and quadricyclane

--Manuscript Draft--

Manuscript Number:	
Article Type:	Full Paper
Corresponding Author:	Julien Bachmann, Ph. D. University of Erlangen Erlangen, GERMANY
Corresponding Author E-Mail:	julien.bachmann@fau.de
Other Authors:	Olaf Brummel
	Daniel Besold
	Tibor Döpper
	Yanlin Wu
	Sebastian Bochmann
	Federica Lazzari
	Fabian Waidhas
	Udo Bauer
	Philipp Bachmann
	Christian Papp
	Hans-Peter Steinrück
	Andreas Görling
	Jörg Libuda
Keywords:	quadricyclane norbornadiene electrochemical IR spectroscopy
Manuscript Classifications:	Electrocatalysis; Energy storage
Suggested Reviewers:	Lifeng Liu lifeng.liu@inl.int Electrochemistry, energy storage
	Jenny Y. Yang j.yang@uci.edu Molecular electrochemistry and energy conversion
	Yogesh Surendranath yogeshs@MIT.EDU Electrochemistry and photoelectrochemistry
	Elizabeth R. Young eyoung@amherst.edu Spectroscopy and electrochemistry of energy-storing molecular systems
Opposed Reviewers:	
Abstract:	We have investigated the electrochemically triggered cycloreversion of quadricyclane (QC) to norbornadiene (NBD), a system that holds the potential to combine both energy storage and conversion in a single molecule. Unambiguous voltammetric traces are obtained for pure NBD and pure QC. The difference in redox potentials is smaller than the energy difference between the neutral molecules. This is due to the energy difference between the corresponding radical cations, as demonstrated by density

	functional theoretical calculations. The vibrational modes of each compound are characterized experimentally in the fingerprint region and identified by DFT methods. Thermal and electrochemical transformations of NBD and QC are monitored in situ by IR spectroelectrochemistry. The kinetics of the cycloreversion of QC to NBD, catalyzed by oxidizing equivalents, is controlled by an applied electrode potential, which implies the ability to adjust in real time the release of thermal power stored in QC.
Author Comments:	Dear Dr. Kemeling, dear members of the editorial board: Please accept the submission of our manuscript entitled „Energy storage in strained organic molecules: Electrochemical and spectroelectrochemical characterization of norbornadiene and quadricyclane", by O. Brummel, D. Besold, T. Döpper, Y. Wu, S. Bochmann, F. Lazzari, F. Waidhas, U. Bauer, P. Bachmann, C. Papp, H.-P. Steinrück, A. Görling, J. Libuda, and J. Bachmann, which we would like to be considered for publication as a full paper in ChemSusChem. All authors have seen the manuscript and approved of its submission. It is not considered for publication elsewhere. In this paper, we present a fundamental electrochemical, photoelectrochemical and theoretical characterization of the pair of valence isomers quadricyclane and norbornadiene, which have been considered as a system in which light energy storage in chemical form is possible upon involvement of one single molecule. All three aspects of the work are novel, as in the past the focus had been put on photophysics and redox-catalytic conversion instead. Our approach is radically new in that we propose the release of the chemical energy in electrical form instead of heat. Towards that long-term goal, we perform a fundamental characterization which demonstrates the electrochemical control of thermal energy release, the spectroscopic monitoring of thermal and electrochemical reactions, and delivers an experimental value for the energy that can be collected in electrical form. We are convinced that this absolutely unique approach will be of high interest to a very wide range of scientists in the energy conversion field, since it represents an original concept that blurs the boundaries between electrochemical and photovoltaic energy conversion, as well as between energy and electrochemical energy transformation, and between energy conversion and energy storage. Thus, ChemSusChem represents the perfect stage for presenting our data. Yours, Julien Bachmann
Section/Category:	
Additional Information:	
Question	**Response**
Dedication	
Submitted solely to this journal?	Yes
Has there been a previous version?	No

Energy storage in strained organic molecules: Electrochemical and spectroelectrochemical characterization of norbornadiene and quadricyclane

Olaf Brummel[1], Daniel Besold[2]†, Tibor Döpper[3], Yanlin Wu[2], Sebastian Bochmann[2], Federica Lazzari[1], Fabian Waidhas[1], Udo Bauer[1], Philipp Bachmann[1], Christian Papp[1], Hans-Peter Steinrück[1,4], Andreas Görling[3,4], Jörg Libuda[1,4]‡, Julien Bachmann[2]§

[1] *Lehrstuhl für Physikalische Chemie II, Friedrich-Alexander-Universität Erlangen-Nürnberg, Egerlandstrasse 3, 91058 Erlangen, Germany*

[2] *Lehrstuhl für Anorganische und Allgemeine Chemie, Friedrich-Alexander-Universität Erlangen-Nürnberg, Egerlandstraße 1, 91058 Erlangen, Germany*

[3] *Lehrstuhl für Theoretische Chemie, Friedrich-Alexander-Universität Erlangen-Nürnberg, Egerlandstrasse 3, 91058 Erlangen, Germany*

[4] *Erlangen Catalysis Resource Center, Friedrich-Alexander-Universität Erlangen-Nürnberg, 91058 Erlangen, Germany*

Abstract

We have investigated the electrochemically triggered cycloreversion of quadricyclane (QC) to norbornadiene (NBD), a system that holds the potential to combine both energy storage and conversion in a single molecule. Unambiguous voltammetric traces are obtained for pure NBD and pure QC, the latter being a strained polycyclic isomer of the former. The difference in redox potentials is smaller than the energy difference between the neutral molecules. This is due to a significant energy difference between the corresponding radical cations, as demonstrated by density functional theoretical (DFT) calculations. The vibrational modes of each pure compound are characterized experimentally in the fingerprint region and identified by DFT methods. Thermal and electrochemical transformations of NBD and QC are monitored in situ by IR spectroelectrochemical methods. The kinetics of the cycloreversion of QC to NBD, which is catalyzed by oxidizing equivalents, can be controlled by an applied electrode potential, which implies the ability to adjust in real time the release of thermal power stored in QC.

Keywords: quadricyclane, norbornadiene, voltammetry, electrochemical IR spectroscopy

†† The first two authors contributed equally to the work.

‡ Also corresponding author, joerg.libuda@fau. de; FAX: +49 9131 8528867

§ Corresponding author: julien.bachmann@fau.de; FAX: +49 9131 8527367

1. Introduction

Today, the capture of light energy is possible in either a photo(electro)chemical or a photovoltaic manner. In the photo(electro)chemical strategy, the fuel generated enables storage and controlled energy release at will. The major difficulty is the complex catalytic reaction network required to transform small stable molecules to their energy-rich counterparts. Indeed, these multistep reactions typically involve major bond rearrangements between several molecules and/or ions, associated with the consecutive transfer of several electrons.[1] The photovoltaic strategy circumvents the issues associated with chemical catalysis but it does not allow for a direct energy storage.[2] We envision that chemical energy storage via intermolecular processes may combine the best of both worlds. Pairs of valence isomers are examples for systems that could combine energy storage and conversion in a single molecule. They could provide a platform for photoelectrochemical energy conversion in which the absence of intermolecular reactions and the minimization of intramolecular atom motion simplifies bond-breaking and bond-making events to their essence, thereby preventing side reactions and rendering the physical phenomenon of electron transfer rate-limiting.

The photochemical conversion of the polycyclic norbornadiene (NBD) (1) to its saturated, strained but metastable, valence isomer quadricyclane (QC) (2) was described over a half-century ago (see **Figure 1**).[3] The reaction of the parent NBD as well as its substituted derivatives proceeds via the triplet state and is typically photosensitized (intramolecularly or intermolecularly), sometimes with quantum yields approaching unity.[4] The reverse reaction releases up to 100 kJ/mol thermally upon adequate triggering, which formally makes the NBD/QC framework a solar fuel.[3c, 4e, 5] As triggers, a variety of mild oxidants open a cycloreversion pathway via the labile $QC^{\bullet+}$ radical cation, which converts to $NBD^{\bullet+}$ along an activationless reaction coordinate.[5a, 6] Research into valence isomers as potential solar fuels peaked in the 1980's when the main limitation of the redox agents as cycloreversion catalysts was recognized: they trigger the energy release by what can be described best as a radical chain mechanism. Naturally, such a process offers a poor degree of control (**Figure 1a**). Not only is this mechanism associated with a number of undesired side-reactions, it also hampers any aspiration of tuning the energy release rate once the radical chain has been set loose.[5b, 6-7]

We envision a scheme in which electrons are given up by QC and taken up by $NBD^{\bullet+}$ with distinct reaction partners. If those partners are electrodes (directly or indirectly), then the chemical strain energy of QC could potentially be converted to electrical energy in a photoelectrochemical device (**Figure 1b**). In fact, this scheme is strongly reminiscent of a dye-sensitized solar cell, with the

potential advantage that in open-circuit configuration, the energy of electrons will not be immediately transferred to the n-type semiconductor and, therefore, will not lost by thermal energy release — in other words, one could imagine that such a device may not only convert solar energy to electrical energy but also store energy chemically if needed.

Unfortunately, only a single paper has been dedicated to the electrochemistry of norbornadiene and quadricyclane to date, without conclusive statements as to oxidation potentials.[8] Conversely, several papers have reported oxidation potentials without showing the data.[9] Thus, as a first step towards the goal presented in **Figure 1** right, the present paper reports on the fundamental electrochemical properties of NBD and QC. We compare various voltammetric methods to determine experimentally the thermodynamic potential difference between the pure $NBD^{\bullet+}$ / NBD and $QC^{\bullet+}$ / QC couples. We follow the electrochemical conversion by means of electrochemical in-situ spectroscopy and characterize the vibrational properties of the reactants and products. Finally, we define procedures for generating clean electrode surfaces unaffected by fouling and demonstrate the electrochemically controlled release of thermal energy from stored QC.

2. Experimental Section

Preparation: Norbornadiene (97% from Alfa Aesar, 2.0 g) and acetophenone (99% from Alfa Aesar, 0.67 g) were stirred with degassed CH_2Cl_2 (p.a. from VWR, 110 mL) in a glass container equipped with a quartz window. The stirred mixture was irradiated for 65 h under nitrogen in the sealed container with a 150-W Osram XBO xenon light source through a cooled water infrared filter. The solvent was evaporatively removed from the reaction mixture to yield and a clear yellowish liquid residue. This residue was then submitted to chromatographic separation over a short silica gel column (pore size 60 Å / 230-400 mesh, 8 cm length, loading 0.25 mL cm^{-2}) with CH_2Cl_2 as the mobile phase. The product was obtained after solvent removal as a clear liquid in 25% yield. ^{1}H-NMR ($CDCl_3$): δ/ppm = 2.02 (t, $^3J_{HH}$ = 1.37 Hz, 2H); 1.48 (m, 4H); 1.36 (m, 2H).

Electrochemical investigation: All measurements were performed with an Interface 1000 from Gamry in a water-jacketed cell (vc-4 from ALS Co., Ltd.) cooled to 18 °C with 4 mL of a degassed electrolytic solution consisting of 5 mM analyte and 0.2 M Bu_4N BF_4 in CH_2Cl_2. The working electrode, auxillary electrode (both platinum) and a pseudo-reference electrode (silver wire) were maintained in a fixed geometry. Potentials were externally referenced before and after measurements to a ferrocene standard electrolyte ($E°$ = 0.46 V vs. SCE).[10] No significant drift of the reference electrode potential was observed over the course of the experiments. Prior to every measurement, the organic

film generated on the working electrode by fouling was removed by 100 voltammetric cycles between –2.5 V and +3.0 V vs. Ag pseudo-reference in a 0.1-M aqueous KCl solution at 1 V s^{-1}.[8]

Electrochemical IR spectroscopy: Electrochemical IR spectra were acquired with a FT-IR spectrometer with evacuated optics (Bruker Vertex 80v). The system features IR optics for electrochemical measurements (Bruker) and a home-built PTFE spectroelectrochemistry cell. For the present experiments, we used a CaF_2 hemisphere (Korth) as the focusing IR window. All spectra were recorded with a liquid-nitrogen-cooled mid-band mercury cadmium telluride (MCT, HgCdTe)-detector. We measured in external reflection mode in a thin layer configuration, i.e. with a few micrometer thick electrolyte layer between the focusing window and the working electrode. All measurements were performed both in p-polarization and in s-polarization, both with an angle of incidence of 60° with respect to the sample normal. The spectral resolution was 2 cm^{-1} and the acquisition time per spectrum was 57 s. Reference spectra of quadricyclane, norbornadiene, acetophenone and acetonitrile were recorded in attenuated total reflection geometry using a germanium hemisphere as ATR window. All Teflon parts and glassware were cleaned in NOCHROMIX® (Sigma Aldrich), rinsed and boiled several times with ultra-pure water (>18 MΩ cm at 25 °C, ≤ 5 ppb TOC) and finally dried under vacuum. The potential was controlled by a commercial potentiostat (Gamry Reference 600). As a quasi-reference electrode (RE) we used a silver wire in a glass tube filled with electrolyte and separated by a frit. Only high purity chemicals were used for the measurements: Acetonitrile (99.999 %, Sigma Aldrich), tetrabutylammonium perchlorate (≥ 99.0 %, Sigma Aldrich), ferrocene (99.5 %, Alfa Aesar), and NBD (98 %, Sigma Aldrich). We used acetonitrile with 0.1 M Bu_4NClO_4 as supporting electrolyte for all in-situ IR spectroscopy measurements. For calibration of the quasi-reference electrode we performed cyclic voltammetry of ferrocene in a separate electrochemical cell with the same electrolyte. All reported potentials shown in this work are referred to the measured ferrocenium / ferrocene couple. As the counter-electrode, a Pt wire was used. As the working electrode, we used a round hat-shaped Pt(111) crystal (MaTeck, 99,999%, depth of roughness <0.01 µm, accuracy of orientation <0.4°), with a surface area of 78.5 mm^2. Before each experiment, the single-crystal electrode was prepared by flame annealing[11], cooled down in Ar/H_2 (~3:1) atmosphere and transferred to the IR cell using a droplet of acetonitrile to protect the surface from the contaminations in air.

DFT calculations: Density-functional calculations were performed using the Turbomole program suite.[12] The exchange-correlation functional of Perdew, Burke, and Ernzerhof (PBE)[13] and the hybrid functional B3LYP[14] were employed in combination with the def2-TZVP and def2-QZVP basis set of Weigend and Ahlrichs.[15]. PBE calculations were accelerated using the RI-J[16] and MARI-J[17] approximations. Additionally the Grimme D3 dispersion correction[18] and the conductor-like

screening model (COSMO)[19] were employed. Vibrational frequencies were calculated within the harmonic approximation and visualized with QVibePlot.[20] While results obtained with different basis sets turned out to be almost identical, PBE energy differences between NBD and QC and between $NBD^{\bullet+}$ and $QC^{\bullet+}$ are 0.33 eV and 0.28 eV, respectively smaller than the B3LYP case. Furthermore, the results obtained with the PBE functional yield a 0.05 eV smaller difference between the oxidation potentials of $NBD^{\bullet+}$/NBD and $QC^{\bullet+}$/QC compared to the B3LYP data.

3. Results and Discussion

a. Preparation and voltammetry

A procedure for a photochemical generation of QC from NBD on a preparative scale has been published.[3b, 21] We suggest using chlorinated hydrocarbons instead of ethereal solvents in order to eliminate the risk of peroxide buildup, on the one hand, and the possibility of using low-cost deuterated solvents, on the other hand. We also find the removal of acetophenone via a short chromatographic separation more practical than distillation. The reaction is monitored most conveniently by nuclear magnetic resonance (NMR) via the disappearance of the alkene resonance of NBD at 6.76 ppm, replaced by signals at 1.48 ppm (cyclopropane protons). The triplet signals of the apical methylene unit are least affected by the transformation (1.99 to 2.02 ppm), whereas the bridgehead protons shift from 3.58 to 1.36 ppm.

The first cyclic voltammogram recorded on a dichloromethane solution of NBD (**Figure 2a**) does not present a distinct maximum. Instead, the curve shape is characteristic of subsequent thermal reactions of the oxidized species. On the reverse scan, the corresponding reduction does not take place, confirming the complete disappearance of $NBD^{\bullet+}$ over the timescale of seconds. These observations are in line with the decomposition of the radical cation, which leads to electrode fouling.[8] We note that due to the organic film that appears upon fouling (and which is impervious to acids, bases and strong oxidants), the working electrode must be cleaned by an electrochemical procedure before each new measurement. Otherwise, the film buildup upon repeated cycling causes an overall current decrease (**Figure 2a**). As a positive ancillary effect, however, the presence of the film also allows the voltammetric peak to emerge relatively clearly from the electrocatalytic background, an observation which indicates that the platinum surface must be catalytically involved in the electrode fouling. The presence of a clear, albeit minor, cathodic peak near +0.2 V, attributed to the reduction of $NBD^{\bullet+}$, demonstrates that despite the decomposition of the radical cation its

lifetime is on the order of seconds. Cyclic voltammograms of QC solutions (**Figure 2b**) share many features of with those of NBD, with the addition of an oxidative shoulder at a less positive potential.

Clearer oxidation peaks can be obtained by pulsed methods such as square wave voltammetry and differential pulse voltammetry (DPV). **Figure 3a** displays DPV curves measured on NBD (red) and QC (green/blue). The former allows one us to determine oxidation potentials accurately. The NBD solution displays a single, well defined (albeit somewhat asymmetric) peak at +1.17 V (vs. the ferrocenium / ferrocene couple in the same electrolyte). The experiment on the QC solution yields two peaks, the first of which is at +0.56 V, whereas the second coincides with that of NBD. Considering that the $QC^{\bullet+}$ radical cation is unstable and immediately converts to $NBD^{\bullet+}$ (**Figure 1a**), we can confidently attribute this peak to the oxidation of NBD itself, formed because at potentials between +0.56 and +1.17 V the $NBD^{\bullet+}$ generated from $QC^{\bullet+}$ is reduced to neutral NBD (either from the electrode pool or from QC in the solution), according to the scheme shown in **Figure 3b**.

We note that these oxidation potential values are in excellent agreement with the published ones.[9, 22] Their difference of 0.61 V corresponds to an energy release of 59 kJ mol^{-1} upon cycloreversion. This number is significantly below the value of ~100 kJ mol^{-1} often cited (see the introduction). The apparent discrepancy is due to the fact that the redox potentials depend not only on the relative energies of both neutral species, but also on those of the oxidized counterparts. The results of our DFT calculations (summarized in **Figure 4**) highlight this aspect. In these calculations, geometry optimizations were carried out for neutral NBD and QC as well as their oxidized counterparts. Dispersion interactions were taken into account by the semiempirical Grimme D3 dispersion correction,[18] whereas the polarizability of the dichlormethane solvent was accounted for by the conductor-like screening model (COSMO) approach[19] (for details, see the experimental section). Not surprisingly, dispersion plays a negligible role, while the polarizability and thus the dielectric constant of the solvent (ε_r = 9.14 for dichlormethane) needs to be considered to obtain accurate energies for the cations. The energy of the latter decreases by 2.03 and 2.05 eV for NBD and QC, respectively, compared to the corresponding vacuum values. For the neutral compounds changes of the energies due to solvent effects are smaller than 0.08 eV. If the redox potential of the Fc^{+}/Fc reference couple of 5.14 V vs. the free electron[10, 23] is subtracted from the calculated ionization energies of 6.03 and 5.43 eV for NBD and QC, respectively, oxidation potentials of 0.89 and 0.29 V result from the four computed energies, values which are in fair agreement with the measured ones at 1.17 and 0.56 V, respectively, given the uncertain difference between the hydrogen and vacuum energy scales.[23b] More importantly, the difference between the computed oxidation potentials of $NBD^{\bullet+}$/NBD and $QC^{\bullet+}$/QC is 0.60 V, essentially in perfect agreement with the measured value of 0.61 V. Thus, the DFT results of **Figure 4** quantify the fraction of thermal energy stored in QC that could potentially be

extracted in electrical form in a scheme such as the one shown by **Figure 1b** to 59% (59 kJ mol^{-1} out of ~100 kJ mol^{-1}) only. The loss is associated with the fact that the radical cations still exhibit an energy difference of 0.44 eV (to be compared to the 1.04 eV difference between the neutral molecules). Both values are in good agreement with the literature.[24]

b. Spectroscopic and spectroelectrochemical monitoring

Now that the thermodynamics of the NBD/QC system are soundly established, let us turn to vibrational spectroscopic methods for following the thermal and electrochemical transformations involving them. To facilitate identification of the reactants by electrochemical in-situ IR spectroscopy, we have investigated the vibrational spectra of NBD and QC both experimentally by attenuated total reflection infrared spectroscopy (ATR IR) and theoretically by density-functional calculations. In **Figure 5a** we compare the experimental and calculated spectra. We focus on the energy region between 1100 and 1600 cm^{-1}, situated between the absorption ranges of the CaF_2 window and the solvent. The bands in this so-called fingerprint region of the hydrocarbon framework are characteristic and particularly favorable to distinguishing between the two isomers. For easier comparison with the experimental data, the calculated spectra are presented after Lorentzian broadening (full width at half maximum of 8 cm^{-1}). Additionally, we visualize the modes corresponding to the most dominant bands in **Figure 5b** using the visualization software QVibeplot.[20] Colored bonds represent changes of the bond length, colored arcs show changes of the bond angles, and the Béziers curves indicate torsions. Different phases are marked with different colors. For further details we refer to the literature.[20]

In general, we find a very good correspondence between the experimental and the calculated spectra. DFT predicts four dominant bands for NBD in this spectral region at 1561, 1295, 1213 and 1185 cm^{-1} which can be associated with the experimentally observed features at 1544, 1311, 1228 and 1204 cm^{-1}, respectively. All values agree well with previous experimental data.[25] The visualization in **Figure 5b** shows that the band at 1544 cm^{-1} (DFT: 1561 cm^{-1}) corresponds to the asymmetrically coupled stretching mode of the two double bonds C_2=C_3 and C_5=C_6, which is polarized along the *x* direction. The band at 1311 cm^{-1} (DFT: 1295 cm^{-1}) is a symmetric C_3-C_4-C_5 deformation/stretching mode antisymmetrically coupled with its C_2-C_1-C_6 counterpart. Whereas the latter mode is *y*-polarized, the antisymmetric C_3-C_4-C_5 deformation/stretching mode at 1204 cm^{-1} (DFT: 1185 cm^{-1}) is polarized along the *x* axis again. The fourth band at 1228 cm^{-1} (DFT: 1213 cm^{-1}) corresponds to a symmetric stretching mode of C_7—C_1 and C_7—C_6. This mode is polarized perpendicular to the 6-membered ring, i.e. along the *z* direction.

In the ATR spectrum of QC we observe two dominant bands at 1256 and 1237 cm^{-1}. Comparison with the calculated spectrum reveals, however, that the band at 1256 cm^{-1} corresponds to an overlapping signal of two modes of different symmetry which are calculated at 1239 and 1238 cm^{-1}. The mode at 1256 cm^{-1} (DFT: 1239 cm^{-1}) is the antisymmetrically coupled C_7—C_1 and C_7—C_6 stretching vibration, polarized along *y*. The mode at 1238 cm^{-1} is a symmetric C—C mode of both cyclopropane rings polarized along *z*. The most intense band at 1237 cm^{-1} (DFT: 1222 cm^{-1}) originates from the antisymmetrically coupled C_2—C_3 and C_5—C_6 (*x*-polarized) stretching mode. This mode is similar to the C_2=C_3 and C_5=C_6 mode at 1544 cm^{-1} in NBD, but appears at much lower frequency in QC because of the transformation of the C=C double bonds into single bonds. This analysis shows that a very detailed picture of the vibrational properties of the QC-NBD couple can be derived in the fingerprint region. Finally, we note that all ATR spectra of synthesized QC samples also show weak features which can be assigned to NBD (marked red and light blue in **Figure 5**). This NBD may originate from incomplete conversion and purification or from back-conversion of a small fraction of QC to NBD during storage and handling.

Next, we investigate the electrochemical oxidation of NBD by in-situ IR spectroscopy. As a working electrode, we use a Pt(111) single crystal. All spectra were acquired in p- and in s-polarization with a 1 M NBD solution in acetonitrile and tetrabutylammonium perchlorate (TBAPC) (0.1 M) as supporting electrolyte. Before the measurement, the quasi-reference electrode was calibrated with respect to the ferrocenium / ferrocene couple and all potentials are given with respect to this reference (V_{fc}). All IR spectra are difference spectra with respect to a reference spectrum recorded at a potential of –0.08 V_{fc}. Subsequently, the potential was increased in steps of 100 mV from –0.08 to +1.87 V_{fc}. In **Figure 6** we show the spectra acquired in the region between 1100 and 1600 cm^{-1}.

Based on our reference experiments and band assignments above, we can identify all four bands in this spectral region as characteristic for NBD. They appear at 1543, 1313, 1228, and 1206 cm^{-1}. The band positions are in good agreement with the ATR spectrum of pure NBD and the small deviations observed are attributed to the solvent effect of acetonitrile. Note that in the difference spectra displayed, positive bands correspond to species which are consumed, whereas negative bands correspond to species which are formed. The positive NBD bands indicate electrooxidation of NBD followed (at least in part) by decomposition. All NBD bands appear at the same potential of 0.7 V_{fc} and the signal intensity increases in parallel with increasing potentials. A comparison with the data in s-polarization (not shown) suggests that the difference signals originate from species in solution and not from species close to the electrode surface. This conclusion is corroborated by the large intensity (large value of $\Delta R/R$) and the absence of a potential-dependent Stark shift, which would be

observed for adsorbed species as a result of the interfacial electrostatic field. Beside the bands of NBD, several positive features can be identified in the region between 1370 and 1450 cm^{-1} which are due to the solvent acetonitrile and a band at 1386 cm^{-1} which can be attributed to the supporting electrolyte TBAPC. Of interest are also a number of negative features below 1150 cm^{-1}, around 1250 cm^{-1} and at 1570 cm^{-1}. Their appearance is correlated with the consumption of NBD. We attribute these bands, which appear in the C—C fingerprint and the C=C stretching region, to ill-defined decomposition products associated with the electrode fouling described in the previous section.

In the next step, we investigate the electrooxidation of QC. To this end, we performed an in-situ IR experiment with 0.1 M QC under conditions otherwise identical to those used above for NBD (acetonitrile, supporting electrolyte TBAPC). The spectra recorded similarly on a solution of QC are displayed in **Figure 7**. The strong bands between 1370 and 1450 cm^{-1} can be assigned to the solvent acetonitrile as discussed above. However, in the region between 1200 and 1350 cm^{-1} we detect several weaker bands associated with NBD and QC. In **Figure 7b** we zoom into this most relevant region. Specifically, we identify the two bands at 1240 cm^{-1} and 1257 cm^{-1}, which are characteristic of QC. Their position agrees well with the ATR-IR reference (**Figure 5**). Both bands appear as positive signals in a potential range between +0.2 and +0.3 V_{fc}, indicating that the corresponding species is consumed. We conclude that this potential range corresponds to the oxidation onset of quadricyclane to $QC^{\bullet+}$, immediately followed by the energy-releasing valence isomerization to $NBD^{\bullet+}$. The subsequent, autocatalytic formation of further NBD (**Figure 1a**, **Figure 3b**) may be followed directly in the in-situ IR spectra. The most intense band of NBD at 1314 cm^{-1} can be identified clearly (blue band in **Figure 7)** as a negative band between +0.2 and +0.5 V_{fc}, indicating the formation of NBD in this potential region. With increasing potential the band intensity remains unchanged up to values of around +0.8 V_{fc}. At higher potentials the signal decreases again and, finally, becomes positive above +1.2 V_{fc}, where NBD itself is oxidized and finally decomposes (see above). Two effects may contribute to the appearance of the positive NBD signals in the limit of high potentials. Firstly, we have to take into account that a small fraction of residual NBD is already present in the pure QC sample either from spontaneous decomposition or from the synthesis (see **Figure 6**). Its oxidation leads to the appearance of a positive signal in the IR difference spectrum. Secondly, some structure appears in the IR spectra at higher potentials, due to the migration of ions and formation of decomposition products which makes the identification of bands more difficult. Above 1.3 V_{fc}, the band at 1314 cm^{-1} remains nearly constant, indicating that the oxidation of norbornadiene is complete. Notably, we observe all bands of QC and of NBD in both s- and p-polarization and no Stark shift is found for any of the features. This indicates that both species are present in solution.

A quantitative analysis of the development of the integrated band intensities as a function of the applied potential is presented in **Figure 8**. To follow the concentrations of the two species as a function of the potential, we use the most intense bands only, i.e. the QC band at 1240 cm^1 (orange curve) and the NBD band at 1314 cm^1 (blue curves). For comparison we also show the band intensities from the electrooxidation experiment with pure NBD (red datapoints, blue curve). From the potential dependence, we observe that the consumption of QC is directly correlated to the formation of NBD (as assumed from **Figure 3**). This implies the ability to control the valence isomerization electrochemically while following the formation of the reaction products in situ by electrochemical IR spectroscopy. From the electrochemical IR experiments we determine the onset and peak potentials for the oxidation of QC as +0.15(±0.1) V_{fc} (onset) and +0.30(±0.1) V_{fc} (peak) and for NBD as +0.9(±0.1) V_{fc} (onset) and +1.1(±0.1) V_{fc}(peak). These onset and peak potentials are shifted with respect to those reported by DPV above (**Figure 3**) due to the higher polarity of the solvent used for the electrochemical experiments (acetonitrile vs. dichloromethane) and transport limitations in the thin film configuration of the IR experiments. Most importantly, however, we find an excellent correspondence of the potential difference $\Delta E_{QC/NBD}$ for the oxidation of QC and NBD of +0.7(±0.2) V determined spectroelectrochemically with the voltammetric values (DPV: +0.61 V, **Figure 3a**), the computed value (DFT: +0.60 V), and the literature.[9]

c. Electrochemical control of the exothermic cycloreversion

We noted above that the electrochemical generation of each $QC^{\bullet+}$ radical cation in solution triggers further cycloreversion of QC to NBD in a catalytic manner. Thus, an electrode held at a certain potential should be able to carry out the catalytic function that has otherwise been fulfilled by the oxidant in the literature by providing a corresponding activity of holes in the electrolytic solution.[26] This is demonstrated by the data of **Figure 9**. The electrochemical currents measured at three potentials near the oxidation potential of QC are quite similar to each other (see **Figure 9a**), and so are the integrated charges passed, correspondingly (diamonds in **Figure 9b**). In contrast to this, the absolute amounts of NBD generated over the course of the experiment and quantified by nuclear magnetic resonance (using the QC starting material as the internal standard, disks in **Figure 9b**) increase drastically when increasing the applied potential. The molar amounts of NBD generated are larger than those of oxidizing equivalents passed at all three potentials, and the ratio between both values is modulated by the working electrode potential. These results are interesting in several respects, from fundamental to applied. Firstly, they demonstrate that an electrode can serve as a reservoir of holes which behave catalytically in the overall non-redox conversion of QC to NBD. Secondly, they imply that the $QC^{\bullet+}$ radical cation has a lifetime sufficient for supporting the radical chain mechanism of the cycloreversion sketched in **Figure 1a**. Thirdly, they signify that an applied

electrode potential can be used to modulate the kinetics of the cycloreversion. In essence, it can be considered as the 'knob' that could be used to control the caloric power output of a QC-based energy storage system.

4. Conclusions

Taken together, our results establish a much-needed experimental knowledge base pertaining to the electrochemical properties of quadricyclane (QC) and norbornadiene (NBD), a couple of valence isomers which allow for the chemical storage of energy in a single-molecular system. Experimental conditions exist in which pure NBD and QC give rise to clean voltammetric signals. Consequently, we now know which fraction of the energy stored in QC can be transformed into electrical form. The vibrational spectroscopy of QC and NBD in the fingerprint region is not only well established experimentally but also exhaustively understood by combining experimental IR spectra with spectra calculated by DFT. In this region, the vibrational spectra allow for straightforward identification of the two species in in-situ experiments. With this infrared spectroelectrochemical tool, the valence isomerization of QC to NBD, as well as subsequent thermal transformations, can be monitored in situ directly. Finally, an electrode can also be utilized as a source of holes generated in the electrolytic solution which catalyze the exothermic conversion of QC to NBD, a reaction which is overall non-redox. The activity of holes in solution, and thereby the caloric power release, can be controlled via the potential applied to the electrode.

These data will enable us and others to explore in more detail how the energy stored in strained valence isomers of polycyclic organic compounds can be released under electrochemical control, or even in electrical form. Certainly, the parent compound NBD itself is not practical as an energy storage platform. Thus, derivatives will have to be designed with appended sensitizers, with improved stability, and with modified thermodynamics on the way towards a practically applicable energy storage system.

Acknowledgments

This work was supported by the Deutsche Forschungsgemeinschaft (DFG) within the Excellence Cluster “Engineering of Advanced Materials” in the framework of the excellence initiative. We acknowledge additional support by the Clariant AG, the European Commission (“chipCAT”, FP7-NMP-2012-SMALL-6, Grant Agreement no. 310191) and by the COST Action CM1104 “Reducible oxide chemistry, structure and function”. The authors are grateful to Marc T. M. Koper (Leiden University) and Jacek Lipkowski (University of Guelph) for great support and many useful discussions. O.B. is particularly thankful to both groups for hosting his research visits.

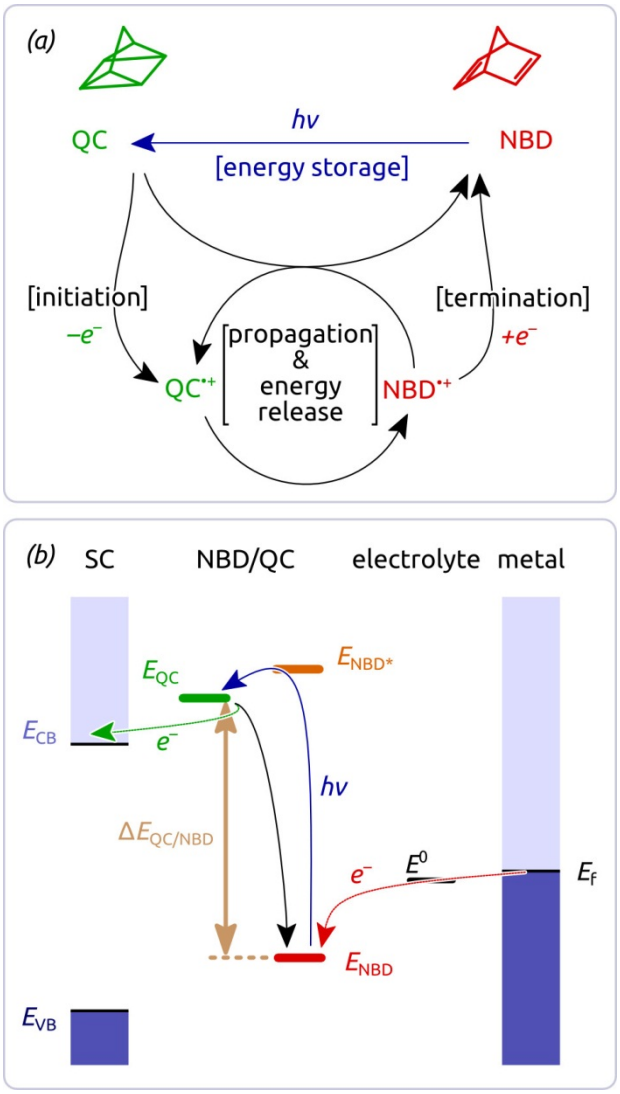

Figure 1. *(a)* Overview of the photochemical, energy-storing conversion of NBD to QC and the redox-mediated, energy-releasing cycloreversion. One recognizes a radical chain mechanism, which offers little opportunity for control. *(b)* Scheme of the proposed photoelectrochemical scheme for controlling the energy release in electrical form.

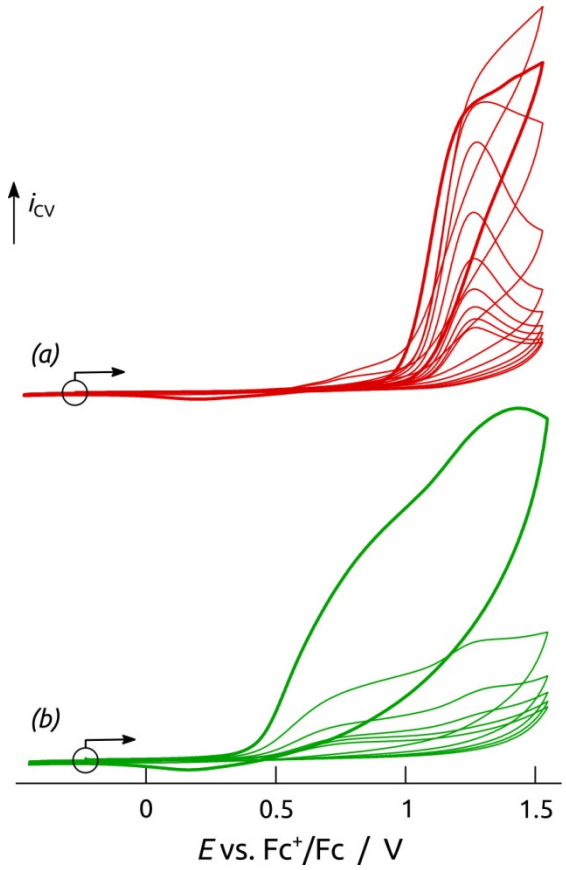

Figure 2. Cyclic voltammetry of *(a)* NBD and *(b)* QC recorded at 20 mV s^{-1} in CH_2Cl_2. The starting point of the measurements is indicated, and the first cycle recorded on a pristine electrode is highlighted with a thicker line.

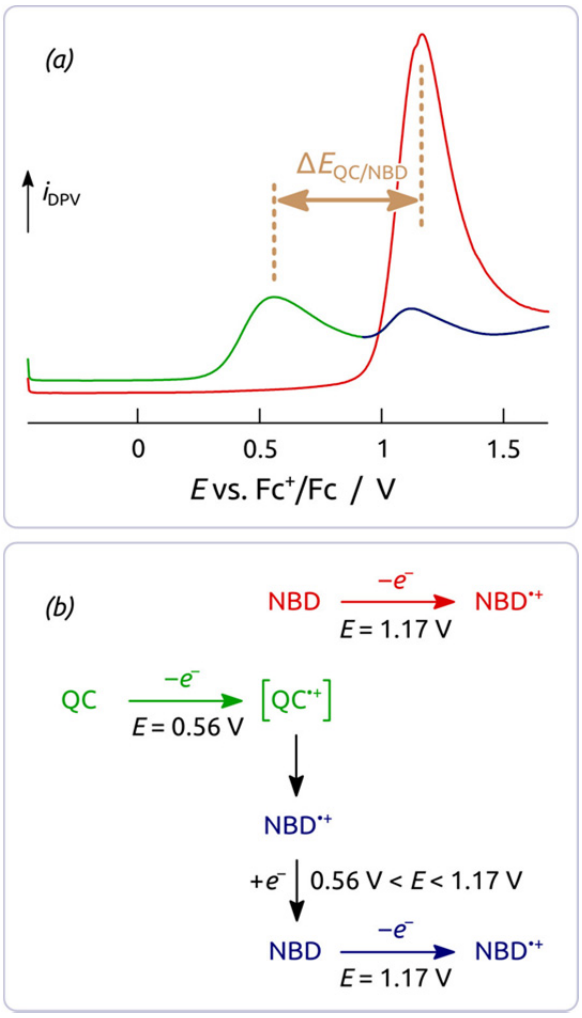

Figure 3. Electrochemical characterization of NBD and QC. *(a)* Differential pulse voltammograms recorded on solutions of pure NBD (red) and QC (green and blue). Parameters: step size 5 mV, pulse size 20 mV, sample period 0.50 s, pulse duration 0.25 s. *(b)* Scheme of the electrochemical and thermal reactions taking place at the electrode surface and in its vicinity.

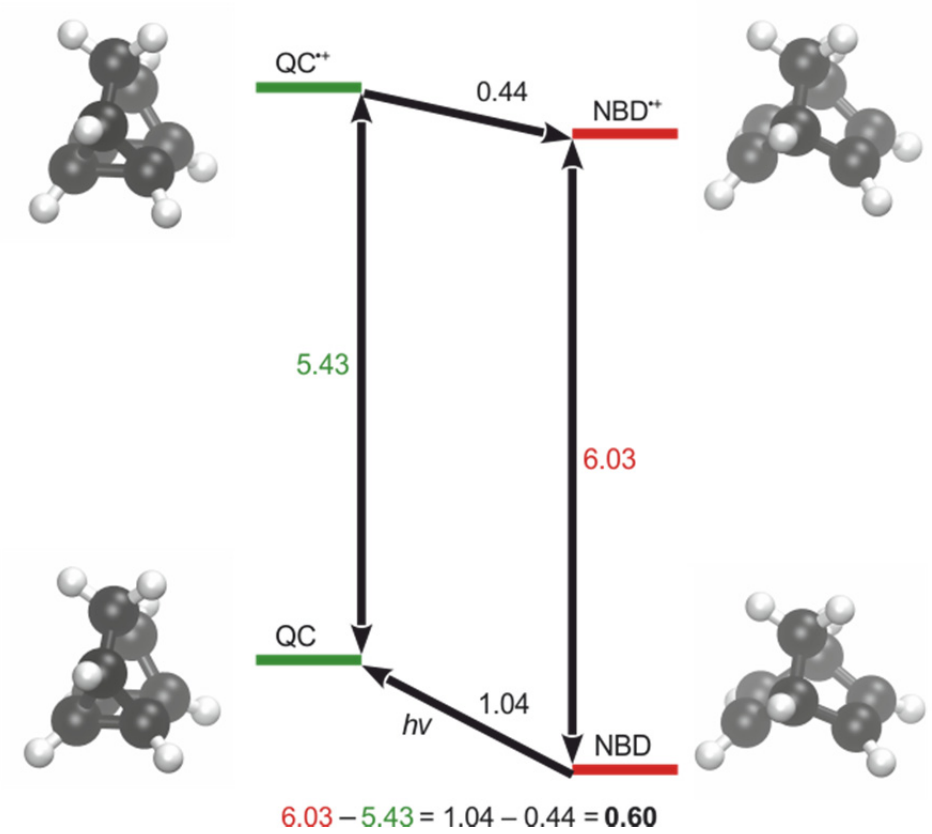

Figure 4. Relative energies in eV and geometries of $QC^{\bullet+}$/QC and $NBD^{\bullet+}$/NBD at the B3LYP/def2-QZVP D3 COSMO (Ɛr = 9.14 for dichloromethane) level of theory.

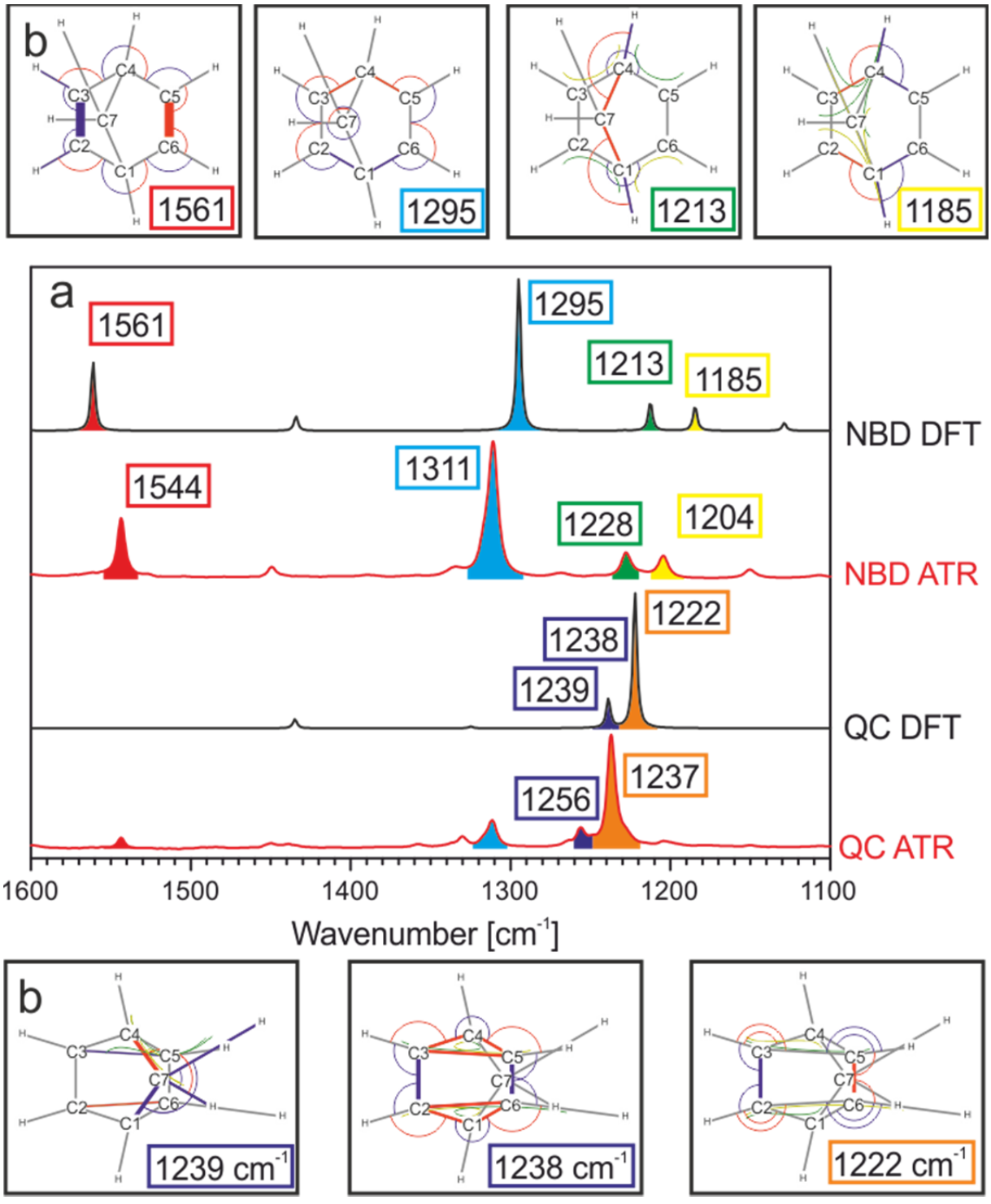

Figure 5. Infrared spectra of QC and NBD in the spectral region from 1100 to 1600 cm^{-1}. (a) Simulated spectra from PBE/def2-TZVP level of theory (black) and experimental (red) IR spectra (ATR) of norbornadiene and quadricyclane. (b) Visualization of the most prominent modes in this spectral region.

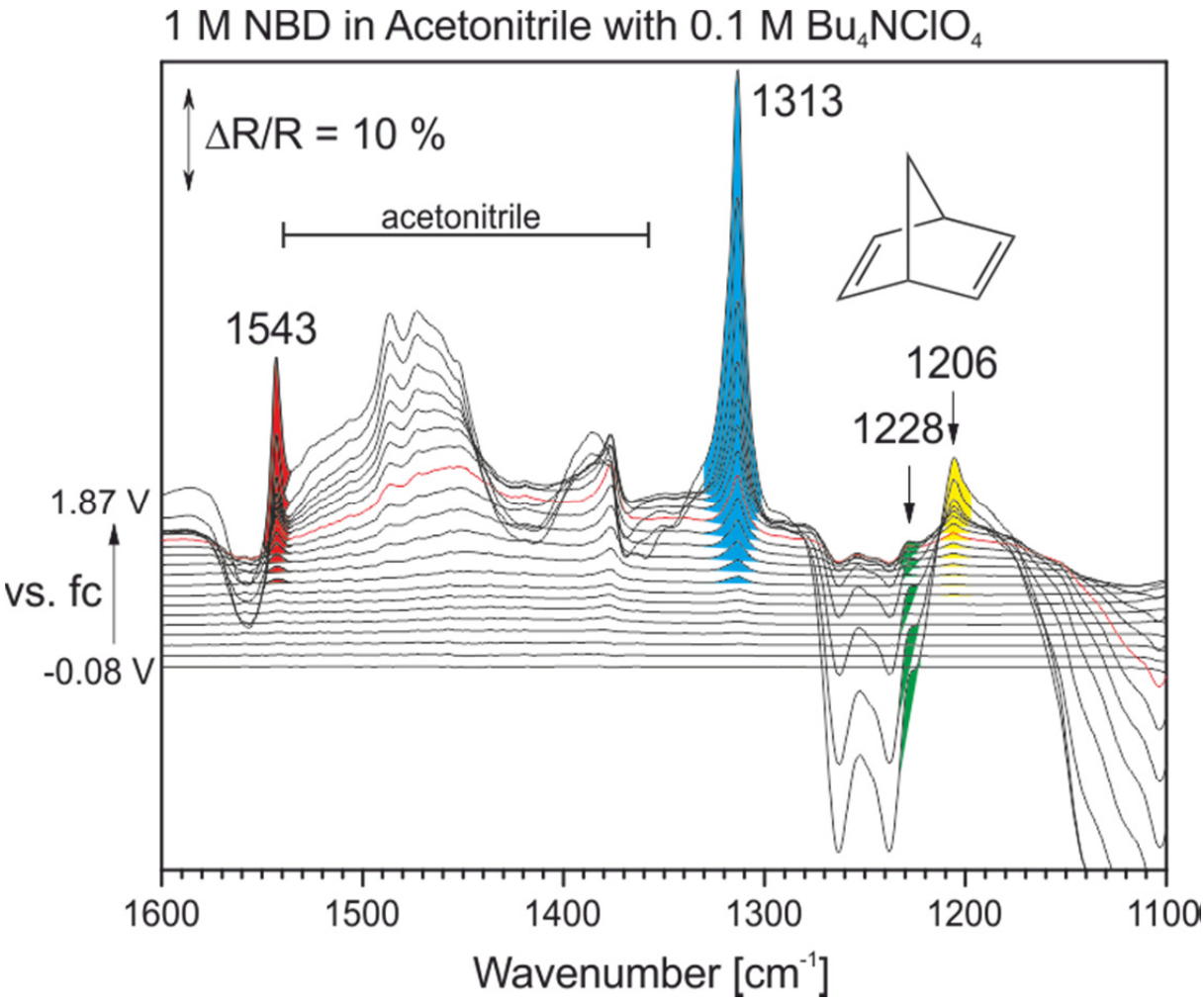

Figure 6. In-situ IR spectra taken during electrochemical oxidation of NBD (1 M) recorded in Bu_4NClO_4 (0.1 M) / acetonitrile . All spectra were taken in p-polarization on a Pt(111) single crystal as a working electrode. The reference spectrum was taken at –0.08 V vs. Fc^+/Fc.

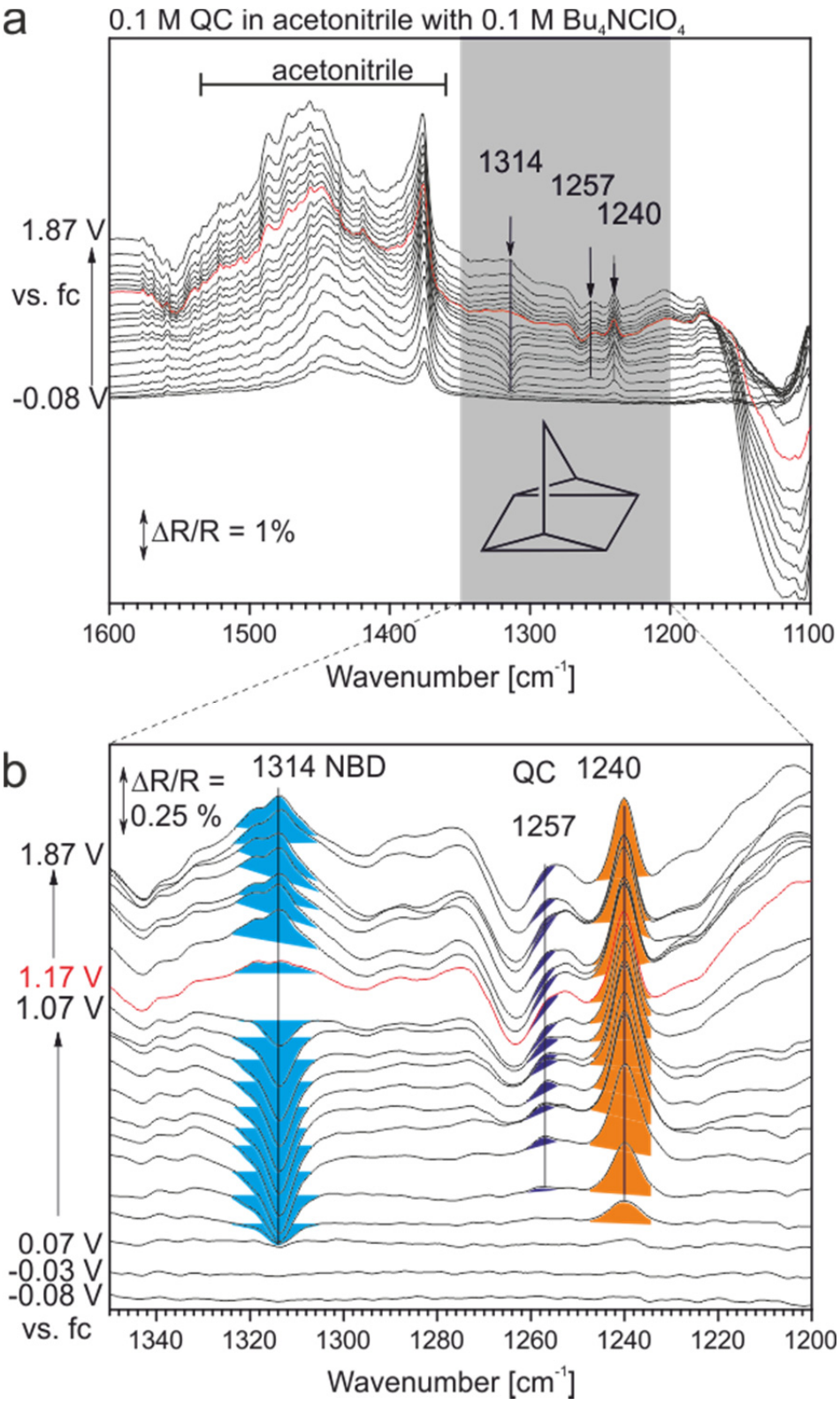

Figure 7. In-situ IR spectra taken during electrochemical oxidation of QC (0.1 M) recorded in Bu_4NClO_4 (0.1 M) / acetonitrile. All spectra were taken in p-polarization on a Pt(111) single crystal as a working electrode. The reference spectrum was taken at –0.08 V vs. Fc^+/Fc. (a) Overview over the spectral region from 1100 to 1600 cm^{-1}; (b) close-up of the spectral region featuring the most prominent bands of QC and NBD.

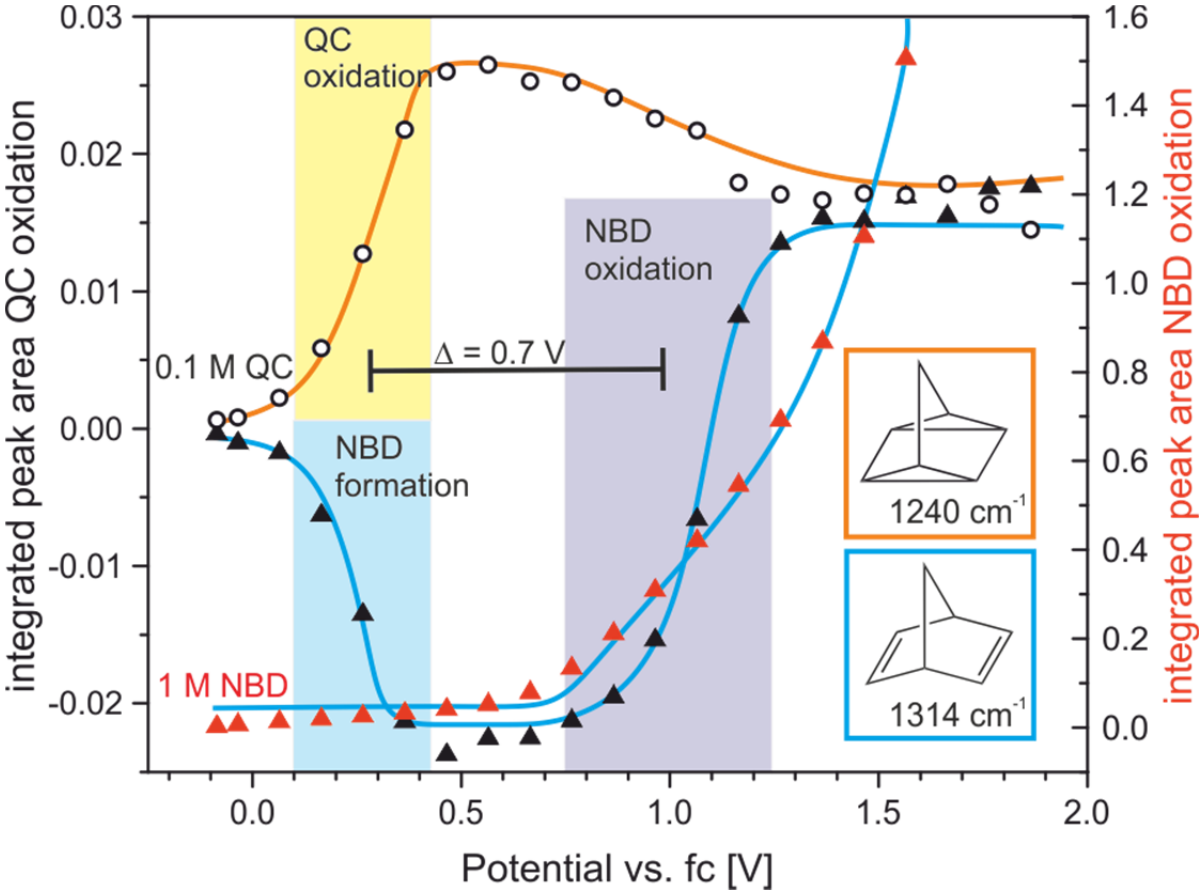

Figure 8. Integrated peak areas of QC and NBD bands in the electrochemical IR spectra taken during the oxidation of 0.1 M quadricyclane (black data points) and 1 M norbornadiene (red data points). The reference spectrum was taken at –0.08 V vs. Fc^+/Fc. The mode at 1240 cm^{-1} (orange curve) corresponds to QC and the mode at 1314 cm^{-1} (blue curves) to NBD.

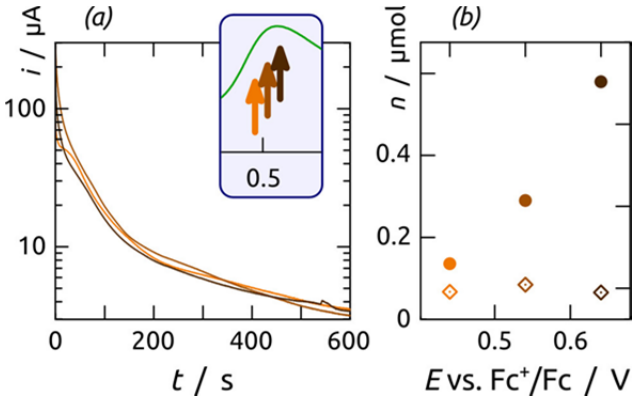

Figure 9. Electrochemical control of cycloreversion kinetics catalyzed by holes. (a) Current-time traces presented for an electrode held for 10 minutes at 0.44, 0.54 and 0.64 V (vs. Fc^+/Fc) in a solution of QC. The inset illustrates where those three potentials are situated with respect to the DPV trace of **Figure 3a**. (b) Comparison of the molar amounts of QC converted to NBD at the three distinct potentials as determined by NMR analysis (disks), compared to the molar equivalent of electrons passed through the electrode during the same period of time (diamonds).

References

[1] S. Y. Reece, J. A. Hamel, K. Sung, T. D. Jarvi, A. J. Esswein, J. J. Pijpers, D. G. Nocera, *Science* **2011**, *334*, 645-648.

[2] aM. Z. Jacobson, *Energy & Environmental Science* **2009**, *2*, 148-173; bR. E. Blankenship, D. M. Tiede, J. Barber, G. W. Brudvig, G. Fleming, M. Ghirardi, M. R. Gunner, W. Junge, D. M. Kramer, A. Melis, T. A. Moore, C. C. Moser, D. G. Nocera, A. J. Nozik, D. R. Ort, W. W. Parson, R. C. Prince, R. T. Sayre, *Science* **2011**, *332*, 805-809.

[3] aS. J. Cristol, R. L. Snell, *Journal of the American Chemical Society* **1958**, *80*, 1950-1952; bW. G. Dauben, R. L. Cargill, *Tetrahedron* **1961**, *15*, 197-201; cD. P. Schwendiman, C. Kutal, *Journal of the American Chemical Society* **1977**, *99*, 5677-5682.

[4] aM. Arenz, V. Stamenkovic, B. B. Blizanac, K. J. Mayrhofer, N. M. Markovic, P. N. Ross, *Journal of Catalysis* **2005**, *232*, 402-410; bA. Cuppoletti, J. P. Dinnocenzo, J. L. Goodman, I. R. Gould, *The Journal of Physical Chemistry A* **1999**, *103*, 11253-11256; cP. A. Grutsch, C. Kutal, *Journal of the American Chemical Society* **1986**, *108*, 3108-3110; dC.-H. Tung, L.-P. Zhang, Y. Li, H. Cao, Y. Tanimoto, *The Journal of Physical Chemistry* **1996**, *100*, 4480-4484; eK. Maruyama, K. Terada, Y. Naruta, Y. Yamamoto, *Chemistry Letters* **1980**, *9*, 1259-1262.

[5] aG. F. Koser, J. N. Faircloth, *The Journal of Organic Chemistry* **1976**, *41*, 583-585; bP. Gassman, in *Strain and Its Implications in Organic Chemistry, Vol. 273* (Eds.: A. de Meijere, S. Blechert), Springer Netherlands, **1989**, pp. 143-167.

[6] K. Maruyama, H. Tamiaki, S. Kawabata, *The Journal of Organic Chemistry* **1985**, *50*, 4742-4749.

[7] E. Durgun, J. C. Grossman, *The Journal of Physical Chemistry Letters* **2013**, *4*, 854-860.

[8] K. White, D. A. Buttry, *Journal of The Electrochemical Society* **2000**, *147*, 266-271.

[9] P. G. Gassman, R. Yamaguchi, G. F. Koser, *The Journal of Organic Chemistry* **1978**, *43*, 4392-4393.

[10] N. G. Connelly, W. E. Geiger, *Chemical Reviews* **1996**, *96*, 877-910.

[11] L. A. Kibler, *Short Course Held at the 51st and 53rd Annual Mtg of the ISE* **2003**.

[12] **2007**, pp. TURBOMOLE V6.5 2013, a development of University of Karlsruhe and Forschungszentrum Karlsruhe GmbH, 1989-2007, TURBOMOLE GmbH, since 2007; available from http://www.turbomole.com.

[13] J. P. Perdew, K. Burke, M. Ernzerhof, *Physical Review Letters* **1996**, *77*, 3865-3868.

[14] A. D. Becke, *The Journal of Chemical Physics* **1993**, *98*, 5648-5652.

[15] F. Weigend, R. Ahlrichs, *Physical Chemistry Chemical Physics* **2005**, *7*, 3297-3305.

[16] F. Weigend, *Physical Chemistry Chemical Physics* **2006**, *8*, 1057-1065.

[17] M. Sierka, A. Hogekamp, R. Ahlrichs, *The Journal of Chemical Physics* **2003**, *118*, 9136-9148.

[18] S. Grimme, J. Antony, S. Ehrlich, H. Krieg, *The Journal of Chemical Physics* **2010**, *132*, 154104.

[19] A. Klamt, G. Schüürmann, *Journal of the Chemical Society, Perkin Transactions 2* **1993**, 799-805.

[20] M. Laurin, *Journal of Chemical Education* **2013**, *90*, 944-946.

[21] C. D. Smith, *Organic Syntheses* **1988**, *50-9*, 962-964.

[22] T. Shono, A. Ikeda, J. Hayashi, S. Hakozaki, *Journal of the American Chemical Society* **1975**, *97*, 4261-4264.

[23] aV. V. Pavlishchuk, A. W. Addison, *Inorganica Chimica Acta* **2000**, *298*, 97-102; bS. Trasatti, *Pure and Applied Chemistry* **1986**, *58*, 955-966.

[24] aD. W. Rogers, F. J. McLafferty, *The Journal of Physical Chemistry A* **1999**, *103*, 8733-8737; bT. Clark, *Acta Chemica Srandinavica* **1997**, *51*, 646-652.

[25] I. W. Levin, W. C. Harris, *Spectrochimica Acta Part A: Molecular Spectroscopy* **1973**, *29*, 1815-1834.

[26] K. Yasufuku, K. Takahashi, C. Kutal, *Tetrahedron letters* **1984**, *25*, 4893-4896.